PERGAMON

PII: S0043-1354(98)00448-5

Wat. Res. Vol. 33, No. 10, pp. 2315–2328, 1999
© 1999 Elsevier Science Ltd. All rights reserved
Printed in Great Britain
0043-1354/99/$ - see front matter

A KINETIC MODEL FOR H_2O_2/UV PROCESS IN A COMPLETELY MIXED BATCH REACTOR

JOHN C. CRITTENDEN[1]*Ⓜ, SHUMIN HU[1], DAVID W. HAND[1]Ⓜ and SARAH A. GREEN[2]

[1]Department of Civil and Environmental Engineering, Michigan Technological University, 1400 Townsend Drive, Houghton, MI 49931, U.S.A. and [2]Chemistry Department, Michigan Technological University, 1400 Townsend Drive, Houghton, MI 49931, U.S.A.

(First received August 1997; accepted in revised form October 1998)

Abstract—A dynamic kinetic model for the advanced oxidation process (AOP) using hydrogen peroxide and ultraviolet irradiation (H_2O_2/UV) in a completely mixed batch reactor (CMBR) is developed. The model includes the known elementary chemical and photochemical reactions, and literature reported photochemical parameters and chemical reaction rate constants are used in this model to predict organic contaminant destruction. Unlike most other kinetic models of H_2O_2/UV oxidation process, the model does not assume that the net formation rate of free radical species is zero (pseudo-steady state assumption). In addition, the model considers the solution pH decrease during the process as mineral acids and carbon dioxide are formed. The model is tested by predicting the destruction of a probe compound, 1,2-dibromo-3-chloropropane (DBCP) in distilled water with the addition of inorganic carbon. The new model developed in this work gives better predictions of the destruction of the target organic compound than the model based on the pseudo-steady state assumption. The model provides a comprehensive understanding of the impact of design and operational variables on process performance. Accordingly the ability of the model to select optimum process variables, such as hydrogen peroxide dosage, is illustrated. © 1999 Elsevier Science Ltd. All rights reserved

Key words—advanced oxidation processes, kinetic model, hydrogen peroxide, ultraviolet irradiation, batch reactor, organic contaminant, radical scavenger

NOMENCLATURE

The following abbreviations are used in this paper:

AdOx™	advanced oxidation model, the computer software for the model developed in this paper
AOP	advanced oxidation process
CMBR	completely mixed batch reactor
DBCP	1,2-dibromo-3-chloropropane
EE/O	electrical energy per order
hv	UV irradiation
ODE	ordinary differential equation
R_1	organic pollutant compound 1
R_2	organic pollutant compound 2
UV	ultraviolet

The following symbols are used in this paper:

b	optical pathlength (cm)
C_a	the concentration of species A (M or mol l^{-1})
C_{ao}	the initial the concentration of species A (M or mol l^{-1})
C_{T,CO_3}	total inorganic carbonate concentration (M or mol l^{-1})
EE/O	electrical energy per order (kWh kgallon^{-1} order^{-1})
f	the fraction of UV irradiation absorbed by a light absorbing species
I_0	incident UV-light intensity (einsteins l^{-1} s^{-1}, or eins. $l^{-1}s^{-1}$)
k	second order reaction rate constant (M^{-1} s^{-1})
k_0	pseudo-first-order rate constant (s^{-1})
k_a	equilibrium constant
r_a	reaction rate of species A in the system (M s^{-1})
t	process operating time (s)
ε	molar extinction coefficient (M^{-1} cm^{-1})
Φ_P	primary quantum yield
Φ_T	overall quantum yield

INTRODUCTION

The H_2O_2/UV advanced oxidation process (AOP) is an attractive alternative to traditional non-

*Author to whom all correspondence should be addressed. [Tel.: +1-906-487-2798; fax: +1-906-487-3292; e-mail address: jcritt@mtu.edu].

destructive water treatment processes (e.g. air stripping, adsorption, membranes) because it can mineralize contaminants from water as opposed merely transporting them from one phase to another. Designing a least cost H_2O_2/UV process for commercial applications requires the determination of important design and operational variables such as the optimum oxidant and irradiation dosages within the reactor. In this study, a mathematical model was developed for this process which can aid engineers in determining these important parameters and determine the fate of the contaminants within the reactor.

According to Peyton (1990), AOPs can be mathematically modeled at several different levels, depending on the known kinetic pathways and reac-

Table 1. The elementary reactions in the H_2O_2/UV AOP system

No.	Reactions	Rate constants, $M^{-1}\,s^{-1}$	Reference
1	$H_2O_2/HO_2^- + h\nu = 2HO^\bullet$	k_1 (measured for the specific system, s^{-1}) or $r_{UV,H_2O_2} = -r_{HOA}/2 = -\Phi_{H_2O_2} I_0 f_{H_2O_2}(1-e^{-A})$ $A = 2.303b(\varepsilon_{H_2O_2} C_{H_2O_2} + \varepsilon_{R_1} C_{R_1} + \varepsilon_{R_2} C_{R_2} + \varepsilon_S C_S + \varepsilon_{HO_2^-} C_{HO_2^-})$ $f_{H_2O_2} = 2.303b(\varepsilon_{H_2O_2} C_{H_2O_2} + \varepsilon_{HO_2^-} C_{HO_2^-})/A$ $\varepsilon_{H_2O_2} = 17.9$–$19.6\ M^{-1}\,cm^{-1}$, $\varepsilon_{HO_2^-} = 228\ M^{-1}\,cm^{-1}$ $\Phi_{H_2O_2} = \Phi_{HO^{2-}} = 0.5$	[a]
2	$H_2O_2 + HO^\bullet = H_2O + HO_2^\bullet$	$k_2 = 2.7 \times 10^7$	Buxton *et al.*, 1988
3	$HO^\bullet + HO_2^- = HO_2^\bullet + OH^-$	$k_3 = 7.5 \times 10^9$	Christensen *et al.*, 1982
4	$H_2O_2 + HO_2^\bullet = HO^\bullet + H_2O + O_2$	$k_4 = 3.0$	Koppenol *et al.*, 1978
5	$H_2O_2 + O_2^{\bullet-} = HO^\bullet + O_2 + OH^-$	$k_5 = 0.13$	Weinslein *et al.*, 1979
6	$HO^\bullet + CO_3^{2-} = CO_3^{\bullet-} + OH^-$	$k_6 = 3.9 \times 10^8$	Buxton *et al.*, 1988
7	$HO^\bullet + HCO_3^- = CO_3^{\bullet-} + H_2O$	$k_7 = 8.5 \times 10^6$	Buxton *et al.*, 1988
8	$HO^\bullet + HPO_4^{2-} = HPO_4^{\bullet-} + OH^-$	$k_8 = 1.5 \times 10^5$	Maruthamuthu *et al.*, 1978
9	$HO^\bullet + H_2PO_4^- = HPO_4^{\bullet-} + H_2O$	$k_9 = 2.0 \times 10^4$	Maruthamuthu *et al.*, 1978
10	$H_2O_2 + CO_3^{\bullet-} = HCO_3^- + HO_2^\bullet$	$k_{10} = 4.3 \times 10^5$	Draganic *et al.*, 1991
11	$HO_2^- + CO_3^{\bullet-} = CO_3^{2-} + HO_2^\bullet$	$k_{11} = 3.0 \times 10^7$	Draganic *et al.*, 1991
12	$H_2O_2 + HPO_4^{\bullet-} = H_2PO_4^- + HO_2^\bullet$	$k_{12} = 2.7 \times 10^7$	Nakashima *et al.*, 1970
13	$HO^\bullet + HO^\bullet = H_2O_2$	$k_{13} = 5.5 \times 10^9$	Buxton *et al.*, 1988
14	$HO^\bullet + HO_2^\bullet = H_2O + O_2$	$k_{14} = 6.6 \times 10^9$	Schested *et al.*, 1968
15	$HO_2^\bullet + HO_2^\bullet = H_2O_2 + O_2$	$k_{15} = 8.3 \times 10^5$	Bielski *et al.*, 1985
16	$HO_2^\bullet + O_2^{\bullet-} = HO_2^- + O_2$	$k_{16} = 9.7 \times 10^7$	Bielski *et al.*, 1985
17	$HO^\bullet + O_2^{\bullet-} = O_2 + OH^-$	$k_{17} = 7.0 \times 10^9$	Beck, 1969
18	$HO^\bullet + CO_3^{\bullet-} = ?$	$k_{18} = 3.0 \times 10^9$	Holeman *et al.*, 1987
19	$CO_3^{\bullet-} + O_2^{\bullet-} = CO_3^{2-} + O_2$	$k_{19} = 6.0 \times 10^8$	Eriken *et al.*, 1985
20	$CO_3^{\bullet-} + CO_3^{\bullet-} = ?$	$k_{20} = 3.0 \times 10^7$	Huie *et al.*, 1990
21	$HO^\bullet + R_1 = ?$	k_{21}	[b]
22	$HO^\bullet + R_2 = ?$	k_{22}	[b]
23	$HO^\bullet + R_1H = ?$	k_{23}	[b]
24	$HO^\bullet + R_2H = ?$	k_{24}	[b]
25	$HO^\bullet + S = ?$	k_{25}	[b]
26	$CO_3^{\bullet-} + R_1 = ?$	k_{26}	[b]
27	$CO_3^{\bullet-} + R_2 = ?$	k_{27}	[b]
28	$HPO_4^{\bullet-} + R_1 = ?$	k_{28}	[b]
29	$HPO_4^{\bullet-} + R_2 = ?$	k_{29}	[b]
30	$O_2^{\bullet-} + R_1 = ?$	k_{30}	[b]
31	$O_2^{\bullet-} + R_2 = ?$	k_{31}	[b]
32	$HO_2^\bullet + R_1 = ?$	k_{32}	[b]
33	$HO_2^\bullet + R_2 = ?$	k_{33}	[b]
34	$R_1 + h\nu = ?$	k_{34} (measured for the specific system, s^{-1}) or $r_{UV,R_1} = -\Phi_{R_1} I_0 f_{R_1}(1-e^{-A})$ $f_{R_1} = 2.303\ b\varepsilon_{R_1} c_{R_1}/A$	[a]
35	$R_2 + h\nu = ?$	k_{35} (measured for the specific system, s^{-1}) or $r_{UV,R_2} = -\Phi_{R_2} I_0 f_{R_2}(1-e^{-A})$ $f_{R_2} = 2.303\ b\varepsilon_{R_2} c_{R_2}/A$	[a]
36	$S + h\nu = ?$	$k_{36} = 0$ (measured for the specific system, s^{-1}) or $r_{UV,S} = -\Phi_S I_0 f_S(1-e^{-A}) = 0$	[c]
37	$H_2CO_3^* \Leftrightarrow H^+ + HCO_3^-$	$pK_{a1} = 6.3$	Stumm *et al.*, 1972
38	$HCO_3^- \Leftrightarrow H^+ + CO_3^{2-}$	$pK_{a2} = 10.3$	Stumm *et al.*, 1972
39	$H_3PO_4 \Leftrightarrow H^+ + H_2PO_4^-$	$pK_{a3} = 2.1$	Stumm *et al.*, 1972
40	$H_2PO_4^- \Leftrightarrow H^+ + HPO_4^{2-}$	$pK_{a4} = 7.2$	Stumm *et al.*, 1972
41	$H_2O_2 \Leftrightarrow H^+ + HO_2^-$	$pK_{a5} = 11.6$	Perry *et al.*, 1981
42	$HO_2A \Leftrightarrow H^+ + O_2A^-$	$pK_{a6} = 4.8$	Perry *et al.*, 1981
43	$R_1H \Leftrightarrow H^+ + R_1$	pK_{a7}	[b]
44	$R_2H \Leftrightarrow H^+ + R_2$	pK_{a8}	[b]

*References: [a]photolysis rate; [b]depends on target organic compound; [c]ignore the humic substance loss from photolysis.

tion rate constants, computer resources available, and the modeling objectives. Compared to other types of mathematical models, a kinetic model gives the most information and provides the best check of the model against actual laboratory data, because all defined or proposed reactions in the system are considered and the rate equations are written for all the main species in solution.

Most kinetic models utilize the pseudo-steady state approximation for the kinetic description of free radical species in the system (Lay, 1989; Glaze *et al.*, 1992; Weir and Sundstrom, 1993; De Laat and Dore, 1994; Glaze *et al.*, 1995; Hong *et al.*, 1996). To invoke the pseudo-steady state approximation, the net formation rates of free radical species are assumed to be zero. Among the kinetic models for the H_2O_2/UV process employing the pseudo-steady state assumption, the model for a completely mixed batch reactor (CMBR) proposed by Glaze *et al.* (1995) and Lay (1989) considered most of the important reactions occurring in the reactor and was verified using a comprehensive experimental study. Their model was able to predict the contaminant concentration as a function of time under different hydrogen peroxide dosages.

Perhaps the most comprehensive kinetic model developed to date was presented by Stefan *et al.* (1996). In the their model, kinetic degradation pathways for the breakdown of acetone to carbon dioxide were proposed and the degradation of acetone (the parent chemical compound) and by-products were predicted by invoking the pseudo-steady state assumption for the formation of radical species.

Yao *et al.* (1992) developed a kinetic model for the H_2O_2/UV process using the ACUCHEM software (Braun *et al.*, 1988) which is available from the National Institute of Standards and Technology (NIST). The kinetic model does not utilize the pseudo-steady state assumption; however, ACUCHEM does have these significant limitations: (1) acid–base equilibrium and variable photolysis rates are not easily considered and (2) complex flow reactor kinetics cannot be considered.

Liao (1993) and Liao and Gurol (1995) developed a kinetic model for a completely mixed flow reactor (CMFR) and they were also able to consider the influence of background organic matter (BOM) on the reactor performance. For a CMFR that is fed with a constant influent concentration, steady state exists and it is possible to invoke the pseudo-steady state assumption for the formation of radical species.

Many of theses studies demonstrated that solution pH has an important impact on the process efficiency (Lay, 1989; Glaze *et al.*, 1995; Liao and Gurol, 1995; Stefan *et al.*, 1996). However, most of the models assumed a constant pH (Lay, 1989; Glaze *et al.*, 1995; Liao and Gurol, 1995; Hu, 1997); and in fact, pH of the solution drops as organic compounds are oxidized into mineral acids, carbon dioxide or acidic intermediates. In this study, we found that the maximum pH change that occurs from degradation of micropollutants in water does not affect the model results significantly in natural water with typical amounts of alkalinity. However, they maybe situations which have high concentrations and low buffer capacity and the change in pH would have to be considered.

The previous kinetic models for the H_2O_2/UV AOP have been applied with different levels of success, but invoking the pseudo-steady state assumption does result in significant errors in some cases. Consequently, a kinetic model with the following improvements is developed as part of this study because this model can be solved in several minutes using a microcomputer and one does not have to evaluate when simplifying assumptions lead to erroneous results: (1) all identified and reasonably proposed photochemical and chemical reactions with regard to the degradation of parent organic compounds are considered; (2) the process kinetics does not employ the pseudo-steady state assumption to simplify the rate expressions; (3) the change in solution pH during the process is considered; and (4) a powerful ordinary differential equation (ODE) solver is utilized to solve the kinetic model equations, a set of very stiff ODEs. The objective of this work is to develop an advanced oxidation model (AdOx™) which is able to predict the degradation of parent organic pollutants and the consumption of hydrogen peroxide in a CMBR. Consequently, the process efficiency under various operating conditions, including initial hydrogen peroxide concentration, UV-light intensity, alkalinity, pH, and the presence of background organic matter, can be evaluated.

THE MECHANISM OF THE H_2O_2/UV OXIDATION PROCESS

Table 1 summarizes all the photochemical and chemical reactions together with literature reported rate constants for those reactions that are common in any H_2O_2/UV process. All photochemical and chemical kinetic parameters as well as rate laws are obtained from independent research reported in the literature (Baxendale and Wilson, 1957; Buxton *et al.*, 1988; Mallard *et al.*, 1992).

The elementary reactions of H_2O_2 photolysis

Early investigations of hydrogen peroxide photolysis (Hunt and Taube, 1952; Baxendale and Wilson, 1957; Volman and Chen, 1959) as well as more recent studies (Schested *et al.*, 1968; Bielski *et al.*, 1977, 1985) have indicated that the following radical chain reactions occur in a hydrogen peroxide solution with UV-light irradiation.

Initiation: (primary photolysis of H_2O_2 or HO_2^-)

$$H_2O_2/HO_2^- + h\nu \longrightarrow 2HO. \quad (1)$$

Propagation:

$$H_2O_2/HO_2^- + HO \longrightarrow H_2O/OH^- + HO_2, \quad (2)$$

$$H_2O_2 + HO_2/O_2 \longrightarrow HO + H_2O/OH^- + O_2. \quad (3)$$

Termination:

$$HO + HO \longrightarrow H_2O_2, \quad (4)$$

$$HO + HO_2/O_2^- \longrightarrow H_2O/OH^- + O_2, \quad (5)$$

$$HO_2 + HO_2/O_2^- \longrightarrow H_2O_2/HO_2^- + O_2. \quad (6)$$

The overall quantum yield (Φ_T) of hydrogen peroxide in this reaction chain is unity at the UV-light wavelength of 254 nm, while the primary quantum yield (Φ_P) of the primary photolysis reaction of hydrogen peroxide (equation 1) at the same wavelength is 0.5.

Reaction mechanism in the presence of target organic pollutants

In the H_2O_2/UV process, hydroxyl radicals produced by the photolysis of hydrogen peroxide quickly react with organic compounds in the solution (reactions (21)–(24) in Table 1). In order to make this kinetic model more widely applicable, it is assumed that there are two pollutant organic compounds (represented by R_1 and R_2) present in the solution. If these organic compounds are acidic compounds, they may exist in both protonated (R_1H and R_2H) and anion forms (R_1^- and R_2^-). In addition to be oxidized by hydroxyl radicals, some organic pollutants may be subject to direct photolysis under UV irradiation as shown by reactions (34) and (35). Some organic pollutants may also be oxidized by superoxide radicals (reactions (30)–(33) in Table 1), or carbonate and phosphate radicals (reactions (26)–(29) in Table 1), of which the formation and loss mechanisms will be described in more detail below.

Reaction mechanism in the presence of other species

In natural waters, there exist various inorganic substances and background organic matter (BOM) which usually reduce the oxidation efficiency of target pollutants by consuming significant amounts of hydroxyl radicals in the H_2O_2/UV system (reactions (6)–(9) and (25) in Table 1). These substances are called hydroxyl radical scavengers since in most cases their reactions with hydroxyl radicals do not yield species that propagate the reaction chain. Carbonate and bicarbonate ions are the most common inorganic hydroxyl radical scavengers in natural waters, while humic substances (represented by S in the reaction pathways) are the most common organic hydroxyl radical scavengers.

The mechanisms of carbonate species scavenging hydroxyl radicals have been investigated by several researchers (Glaze and Kang, 1988, 1989a,b; Peyton and Glaze, 1988). Carbonate and bicarbonate ions (CO_3^{2-}/HCO_3^-) react with hydroxyl radicals to produce carbonate radicals, $CO_3^{\cdot -}$ and $HCO_3^{\cdot}$ (reactions (6) and (7) in Table 1), which are reported to be similarly active and therefore can be referred to as one term, $CO_3^{\cdot -}$ (Chen and Hoffman, 1975; Larson and Zepp, 1988). In general, the most significant reaction of $CO_3^{\cdot -}$ is to react with hydrogen peroxide forming superoxide radicals, $HO_2^{\cdot}$ (reactions (10) and (11) in Table 1, Peyton and Glaze, 1988). $CO_3^{\cdot -}$ also reacts with hydroxyl radicals and other free radicals (reactions (18)–(20) in Table 1). Since $CO_3^{\cdot -}$ is a weak oxidant, it may react with some target organic compounds (reactions (26) and (27)). But for the treatment of most organic pollutants, these reactions are insignificant and can be ignored. The role of phosphate ions in the H_2O_2/UV process is similar to that of carbonate ions as represented by reactions (8), (9) and (12) (Peyton *et al.*, 1987).

Humic substances impact the process efficiency by absorbing UV-light, which reduces the photolysis of hydrogen peroxide (reaction (36) in Table 1), as well as by scavenging hydroxyl radicals (reaction (25) in Table 1). The AdOx™ model does not consider the influence of the by-products which are formed from both of the above mechanisms, and the degradation of humic substances from photolysis is ignored (i.e., assume $r_{s,UV} = 0$). However, the AdOx™ model accounts for the reduction of the hydrogen peroxide photolysis, as well as target organic compounds photolysis, due to light absorption by humic substances (see the photolysis rate expressions for the photolytic reactions (1), (34), and (35) in Table 1). This approach has been used successfully by Liao (1993) and Liao and Gurol (1995) and Hu (1997).

MODEL EQUATIONS

Governing equation in a CMBR

The mass balance for a species, A, in a completely mixed batch reactor (CMBR) yields the following ordinary differential equation:

$$\frac{dC_a}{dt} = r_a, \quad C_a\big|_{t=0} = C_{a0} \quad (7)$$

in which C_{a0} is the influent concentration of species A, C_a is the concentration of A at time t, and r_a is the overall kinetic rate expression of the species A in the reaction system.

Kinetic rate expressions

Based on the reactions in Table 1, the overall kinetic rate expressions can be written for inclusion in equation 7. These species include: H_2O_2/HO_2^-, HO, $HO_2^{\cdot}/O_2^{\cdot -}$, $CO_3^{\cdot -}$, HCO_3^-/CO_3^{2-}, $HPO_4^{\cdot -}$, $H_2PO_4^-/HPO_4^{2-}$, R_1 (or R_1^-/R_1H), R_2 (or R_2^-/R_2H), and S,

$$r_{H_2O_2} = r_{UV,H_2O_2}(-k_1[H_2O_2]) - k_2[H_2O_2][HO] - k_3[HO_2^-][HO] - k_4[H_2O_2][HO_2] - k_5[H_2O_2][O_2^-] - k_{10}[H_2O_2][CO_3^-] - k_{11}[HO_2^-][CO_3^-] - k_{12}[H_2O_2] \times [HPO_4^-] + k_{13}[HO][HO] + k_{15}[HO_2] \times [HO_2] + k_{16}[HO_2][O_2^-], \quad (8)$$

$$r_{HO} = r_{UV,OH}(+2k_1[H_2O_2]) - k_2[H_2O_2][HO] - k_3[HO][HO_2^-] + k_4[H_2O_2][HO_2] + k_5[H_2O_2][O_2^-] - k_6[HO] - k_6[HO] \times [CO_3^{2-}] - k_7[HO][HCO_3^-] - k_8[HO] \times [HPO_4^{2-}] - k_9[HO][H_2PO_4^-] - k_{13}[HO] \times [HO] - k_{14}[HO][HO_2] - k_{17}[HO][O_2^-] - k_{18}[HO][CO_3^-] - k_{21}[HO][R_1] - k_{22}[HO][R_2] - k_{23}[HO][R_1H] - k_{24}[HO][R_2H] - k_{25}[HO][S], \quad (9)$$

$$r_{HO_2} = k_2[H_2O_2][HO] + k_3[HO_2^-][HO] - k_4[HO_2][H_2O_2] - k_5[O_2^-][H_2O_2] + k_{10}[H_2O_2][CO_3^-] + k_{11}[CO_3^-][HO_2^-] + k_{12}[H_2O_2][HPO_4^-] - k_{14}[HO_2][HO] - k_{15}[HO_2][HO_2] - k_{16}[HO_2][O_2^-] - k_{17}[O_2^-][HO] - k_{19}[O_2^-][CO_3^-] - k_{30}[O_2^-][R_1] - k_{31}[O_2^-][R_2] - k_{32}[HO_2][R_1] - k_{33}[HO_2][R_2], \quad (10)$$

$$r_{CO_3^-} = k_6[HO][CO_3^{2-}] + k_7[HO][HCO_3^-] - k_{10}[CO_3^-][H_2O_2] - k_{11}[CO_3^-] \times [HO_2^-] - k_{18}[CO_3^-][HO] - k_{19}[CO_3^-][O_2^-] - k_{20}[CO_3^-][CO_3^-] - k_{26}[CO_3^-][R_1] - k_{27}[CO_3^-][R_2], \quad (11)$$

$$r_{HCO_3^-} = -k_6[CO_3^{2-}][HO] - k_7[HCO_3^-][HO] + k_{10}[CO_3^-][H_2O_2] + k_{11}[CO_3^-] \times [HO_2^-] + k_{19}[CO_3^-][O_2^-], \quad (12)$$

$$r_{HPO_4^-} = k_8[HO][HPO_4^{2-}] + k_9[HO][H_2PO_4^-] - k_{12}[HPO_4^-][H_2O_2] - k_{28}[HPO_4^-] \times [R_1] - k_{29}[HPO_4^-][R_2], \quad (13)$$

$$r_{H_2PO_4^-} = -k_8[HPO_4^{2-}][HO] - k_9[H_2PO_4^-][HO] + k_{12}[HPO_4^-][H_2O_2], \quad (14)$$

$$r_{R_1} = -k_{21}[R_1][HO] - k_{23}[R_1H][HO] - k_{26}[R_1] \times [CO_3^-] - k_{28}[R_1][HPO_4^-] - k_{30}[R_1] \times [O_2^-] - k_{32}[R_1][HO_2] + r_{UV,R_1}(-k_{34}[R_1]), \quad (15)$$

$$r_{R_2} = -k_{22}[R_2][HO] - k_{24}[R_2H][HO] - k_{27}[R_2] \times [CO_3^-] - k_{29}[R_2][HPO_4^-] - k_{31}[R_2] \times [O_2^-] - k_{33}[R_2][HO_2] + r_{UV,R_2}(-k_{35}[R_2]), \quad (16)$$

$$r_S = -k_{25}[S][HO] + r_{UV,S}(-k_{36}[S]). \quad (17)$$

The solution pH is calculated during the integration based on solution charge balance assuming the destroyed parent compounds are completely converted into carbon dioxide (or strictly speaking, H_2CO_3*) and mineral acids.

The simultaneous ordinary differential equations that result from the substitution of the above rate equations 8–17 into the governing equation 7 were solved using a backward differentiation formula method (Gear's method) called DGEAR. DGEAR and the associated nuclei are adaptations of a package designed by Hindmarsh based on Gear's subroutine DIFSUB (Hindmarsh, 1974).

MODEL VERIFICATION – OXIDATION OF DBCP IN A CMBR

Glaze *et al.* (1995) proposed a kinetic model for the oxidation of organic contaminants using the H_2O_2/UV process in a CMBR. Their model was compared to laboratory experimental results for a probe compound, 1,2-dibromo-3-chloropropane (DBCP) (Lay, 1989). The laboratory study was conducted in a cylindrical 70-l (liquid volume) reactor that had a 33-cm o.d. The UV radiation was provided by one to four low-pressure mercury lamps (8.4 W at 254 nm each) symmetrically located in the

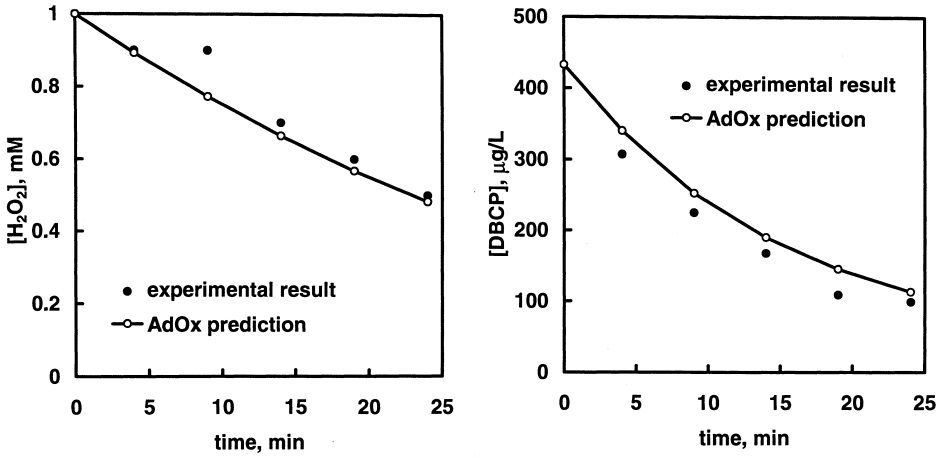

Fig. 1. The comparison between AdOx model prediction and experimental result for one experiment (operating parameters: $[H_2O_2] = 1.00$ mM, $[DBCP]_0 = 1.83\ \mu$M, $C_{T,CO_3} = 4$ mM, pH 8.4, $I_0 = 1.04 \times 10^{-6}$ eins./l s).

reactor. The optical path length of the system was determined to be 15.8 cm. The UV-light intensity (I_0) at 254 nm for one, two, three, and four lamps in the reactor was measured to be 0.26, 0.52, 0.77, and 1.04×10^{-6} eins./l s, respectively.

As stated previously, AdOx™ does not assume the net rate of production of radical species is zero, whereas the kinetic model of Glaze *et al.* (1995) did. In addition, AdOx™ addresses more chemical reactions and includes light absorption by background organic matter (BOM). The pH change of the solution is predicted assuming that the parent compound, DBCP, is completely converted into mineral acids (HCl and HBr) and carbon dioxide. (This assumption would yield the largest impact of pH change on the model predictions.) The assumption appears to be valid based on the experimental observation of Lay (1989) that the loss of DBCP corresponded to appropriate stoichiometric increases in bromide and chloride ions, and only a trace of chloracetic acid and other by-products were detected. Similar observations were reported by Milano *et al.* (1990).

The experimental data from the modeling study of Glaze *et al.* (1995) was used to verify the AdOx™ model (the consideration of BOM will not be verified in this modeling study). The following parameters reported by Lay (1989) and Glaze *et al.* (1995) are used in this modeling study. The second order rate constant between DBCP and hydroxyl radicals is $1.5 \times 10^8\ M^{-1}\ s^{-1}$ (k_{21}); the molar extinction coefficient and the photolysis quantum yield of DBCP at the wavelength of 254 nm are $14.7\ M^{-1}\ cm^{-1}$ (ε_{DBCP}) and 0.49 (Φ_{DBCP}), respectively. The rate constants for reactions between DBCP and other radicals ($CO_3^{\cdot -}$, $O_2^{\cdot -}$, and $HO_2^{\cdot}$) are all assumed to be negligible as compared to HO.

Figure 1 demonstrates that AdOx™ can accurately predict the DBCP and hydrogen peroxide data from Lay (1989) for one experiment. Similar agreements are found for other experiments. If the DBCP data is plotted as $\ln(C/C_0)$ vs reaction time, the data falls on a straight line. This means the degradation of DBCP in the H_2O_2/UV process follows a pseudo-first order kinetics,

$$\ln\left[\frac{C}{C_0}\right] = -k_0 t, \tag{18}$$

in which C and C_0 are the concentrations of DBCP at any time t and initial time, respectively; and k_0 is the pseudo-first order rate constant for overall degradation rate of DBCP. Consequently, the comparisons between model predictions and experimental results will be expressed in terms of pseudo-first order rate constants, k_0. The measured k_0 and the predicted values for DBCP from both the model of Glaze *et al.* (1995) and the AdOx™ model are compared in Table 2 and Figs 2–6. In Table 2, $\Delta\%$ represents the residual between the calculated k_0 from AdOx™ and experimental data.

$$\Delta\% = 100 \times \frac{k_{AdOx} - k_{experiment}}{k_{experiment}}. \tag{19}$$

The average residual value for all experiments is 13.6%. AdOx™ gives a better prediction for most of the experiments as compared to the model of Glaze *et al.* (1995) that utilizes the pseudo-steady state assumption and constant pH assumption.

The impact of assuming pseudo-steady-state and constant pH for several cases are compared in Table 3. The two assumption model in Table 3 assumes that both assumptions are valid. The constant pH model does not assume pseudo-steady-state. The AdOx™ model predicts the pH change and does not utilize the pseudo-steady-state assumption. According to Table 3, the pseudo-steady-state assumption has the greatest impact on the pseudo-first order rate constant. As expected, the rate is lower when the pseudo-state-state

Table 2. Comparison of experimental measured, Glaze et al.'s model predicted, and AdOx™ model predicted pseudo-first-order rate constants of DBCP degradation

$[R_0]$ (μM)	$[H_2O_2]$ (mM)	I_0 (eins./l s)	$[C_{T,CO_3}]$ (mM)	pH	k_0 ($\times 10^5$ s^{-1})				EE/O (kWh/kgallon-order)	
					Glaze et al.'s model	experiment	AdOx™ model	Δ (%)	experiment	AdOx™ model
Group I (changing $[H_2O_2]_0$)										
1.63	0.054	1.04×10^{-6}	4	8.4	4	26.5	34.2	29.0	14.6	11.3
1.43	0.096	1.04×10^{-6}	4	8.3	8	30.7	39.2	27.7	12.6	9.90
1.42	0.35	1.04×10^{-6}	4	8.4	15	61.9	64.7	4.5	6.30	6.00
1.55	0.56	1.04×10^{-6}	4	8.5	24	81.5	80.4	−1.3	4.77	4.83
1.83	1	1.04×10^{-6}	4	8.4	56	106	101.4	−1.5	3.67	3.83
1.77	1.5	1.04×10^{-6}	4	8.4	70	108	111.9	3.6	3.60	3.47
1.5	3	1.04×10^{-6}	4	8.4	81	107	107.7	0.7	3.63	3.60
1.52	4.4	1.04×10^{-6}	4	8.4	74	85.5	92.0	7.6	4.53	4.20
3.06	6.6	1.04×10^{-6}	4	8.5	58	70.9	71.1	0.3	5.47	5.47
Group II (changing $[H_2O_2]_0$)										
1.11	0.26	1.04×10^{-6}	0.1	8.1	236	258	228.4	−11.5	1.50	1.70
1.47	0.5	1.04×10^{-6}	0.1	8.4	267	272	244.2	−10.2	1.43	1.60
1.35	0.79	1.04×10^{-6}	0.1	8.0	274	271	241.9	−10.7	1.43	1.60
1.32	1.5	1.04×10^{-6}	0.1	8.2	236	229	220.5	−3.7	1.70	1.77
1.14	3	1.04×10^{-6}	0.1	8.2	172	160	165.1	3.2	2.43	2.33
Group III (changing $[H_2O_2]_0$)										
1.81	0.27	0.52×10^{-6}	4	8.3		18.9	31.6	67.2	10.3	6.13
2.08	0.54	0.52×10^{-6}	4	8.3		23.7	43.2	82.3	8.17	4.50
1.23	1	0.52×10^{-6}	4	8.4		52.5	53.7	2.3	3.70	3.60
1.33	1.5	0.52×10^{-6}	4	8.4		55.9	57.8	3.4	3.47	3.37
1.18	3	0.52×10^{-6}	4	8.5		45.8	53.7	17.2	4.23	3.60
1.16	3.85	0.52×10^{-6}	4	8.3		41.5	48.8	17.6	4.47	3.97
1.8	6	0.52×10^{-6}	4	8.2		26.8	37.7	40.7	7.23	5.13
Group IV (changing I_0)										
1.38	1	0.26×10^{-6}	4	8.4		30.2	27.8	−7.9	3.20	3.50
1.23	1	0.52×10^{-6}	4	8.4		52.5	53.7	2.3	3.70	3.60
1.16	1	0.77×10^{-6}	4	8.4		75.7	77.3	2.1	3.83	3.77
1.83	1	1.04×10^{-6}	4	8.4		106	101.4	−1.5	3.67	3.83
Group V (changing I_0)										
1.09	1.5	0.26×10^{-6}	4	8.4		25.3	29.5	16.6	3.83	3.30
1.33	1.5	0.52×10^{-6}	4	8.4		55.9	57.8	3.4	3.47	3.37
1.44	1.5	0.77×10^{-6}	4	8.4		82.7	84.2	1.8	3.50	3.47
1.77	1.5	1.04×10^{-6}	4	8.4		108	111.9	3.9	3.60	3.47
Group VI (changing C_T)										
2.34	1	1.04×10^{-6}	0.01	7.2		228	285.6	25.3	1.70	1.37
1.91	1	1.04×10^{-6}	1	8.1		179	171.6	−4.1	2.17	2.27
1.42	1	1.04×10^{-6}	2	8.4		150	137.7	−8.2	2.60	2.80
1.83	1	1.04×10^{-6}	4	8.4		106	101.4	−1.5	3.67	3.83
Group VII (changing pH)										
1.01	1	1.04×10^{-6}	4	10.4		23.7	27.5	16.0	16.4	13.5
1.04	1	1.04×10^{-6}	4	9.4		36.1	46.5	28.8	10.7	8.03
1.83	1	1.04×10^{-6}	4	8.4		106	92.8	−12.5	3.67	3.83
1.02	1	1.04×10^{-6}	4	7.4		132	119.3	−9.6	2.93	3.13
1.15	1	1.04×10^{-6}	4	6.4		196	160.4	−18.2	1.97	2.33
1.32	1	1.04×10^{-6}	4	5.4		219	243.3	11.1	1.77	1.53

assumption is invoked because the hydroxyl radical species concentration is higher when it is not invoked. In addition, the rate constant is slightly higher when pH is allowed to decreased as the result of acid production. There is a difference between "the two-assumption model" and the model of Glaze *et al.* (1995) which is reported in Table 2, and this may due to the differences in reaction mechanisms and ODE solvers used in the computation programs.

The performance of AdOx™ under various conditions as well as an analysis of the effects of differ-

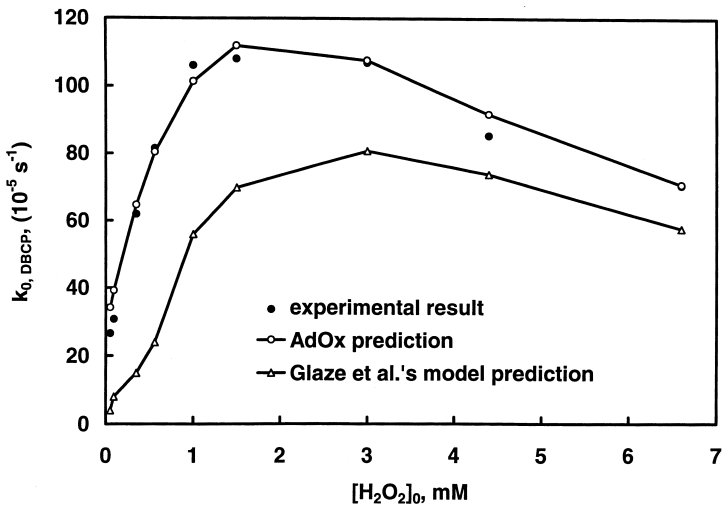

Fig. 2. Effect of initial hydrogen peroxide concentration on the pseudo-first-order rate constant for the oxidation of DBCP (operating parameters: $C_{T,CO_3} = 4$ mM; $I_0 = 1.04 \times 10^{-6}$ eins./l s).

ent operating conditions on the treatment efficiency of the H_2O_2/UV process are discussed in more detail below.

Effect of initial hydrogen peroxide concentration on DBCP degradation

The data from the experimental groups I-III (see Table 2) reveal the effect of the initial hydrogen peroxide concentration on the performance of the H_2O_2/UV process for various total inorganic carbonate concentrations and different incident UV-light intensities. These effects are also illustrated in Figs 2–4. At low initial hydrogen peroxide concentration levels, increasing the hydrogen peroxide concentration increases the DBCP degradation rate. However, when the hydrogen peroxide concentration becomes high, the excess hydrogen peroxide consumes hydroxyl radicals as indicated by reactions (2) and (3), and the DBCP degradation rate decreases. Consequently, for a given light intensify, there is an optimum hydrogen peroxide concentration with regard to the organic pollutant removal efficiency of the H_2O_2/UV process.

As can be seen from Figs 2 to 4, AdOx™ predicts the experimental observations very well for most of the experiments. In the case of low intensity UV irradiation ($I_0 = 0.52 \times 10^{-6}$ eins./l s, AdOx™ predictions for high or low H_2O_2 concentrations ($[H_2O_2]_0 \leq 0.54$ mM, or $[H_2O_2]_0 = 6$ mM) do not agree with observations as shown in Fig. 4. Under these conditions, the hydroxyl radical concentration is low and the direct photolysis of DBCP becomes the principal mechanism of DBCP decomposition. The disagreement between the model predictions and observations under these situations may be due

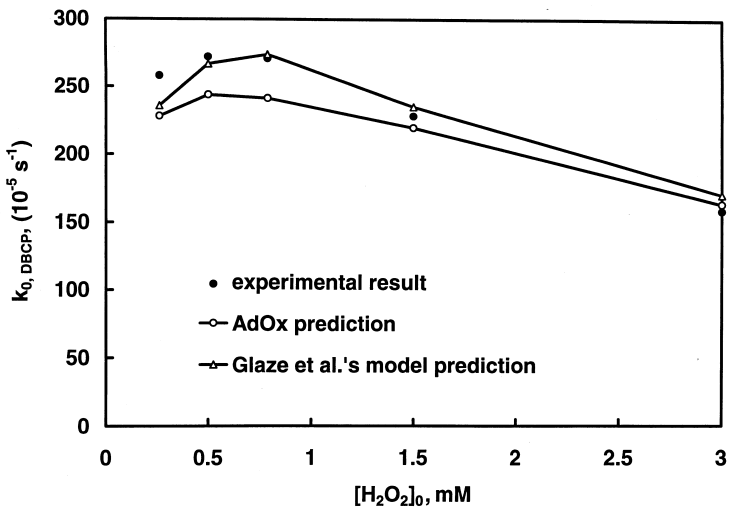

Fig. 3. Effect of initial hydrogen peroxide concentration on the pseudo-first-order rate constant for the oxidation of DBCP (operating parameters: $C_{T,CO_3} = 0.1$ mM; $I_0 = 1.04 \times 10^{-6}$ eins./l s).

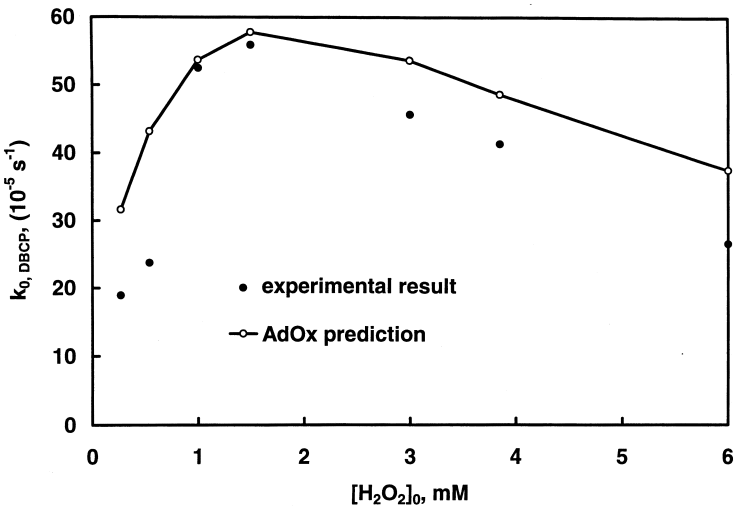

Fig. 4. Effect of initial hydrogen peroxide concentration on the pseudo-first-order rate constant for the oxidation of DBCP (operating parameters: $C_{T,CO_3} = 4$ mM; $I_0 = 0.52 \times 10^{-6}$ eins./l s).

to an inaccurate estimation of the photochemical parameters of DBCP, i.e., ε_{DBCP} and Φ_{DBCP}.

Effect of initial hydrogen peroxide concentration on H_2O_2 consumption

According to Beer–Lambert law and the definition of overall quantum yield, under UV irradiation, the overall photolysis rate of a pure hydrogen solution can be expressed as follows:

$$r_{H_2O_2} = -\Phi_T I_0 (1 - e^{-D}), \tag{20}$$

$$D = 2.303 \varepsilon b [H_2O_2], \tag{21}$$

in which Φ_T is the overall quantum yield of hydrogen peroxide, I_0 is the incident UV-light intensity, ε is the molar extinction coefficient of hydrogen peroxide at the irradiation wavelength, b is the optical path length of the system, $[H_2O_2]$ is the hydrogen peroxide concentration; D is the optical density of the system, which primarily depends on hydrogen peroxide concentration. The rate expression can be simplified when D is very small or very large as follows.

When D is small, the decomposition of hydrogen peroxide follows a first order kinetics,

$$r_{H_2O_2} = -\Phi_T I_0 (1 - e^{-D}) \approx -\Phi_T I_0 D$$
$$= -2.303 \varepsilon b \Phi_T I_0 [H_2O_2]. \tag{22}$$

While when D is large, it is zero order,

$$r_{H_2O_2} = -\Phi_T I_0 (1 - e^{-D}) \approx -\Phi_T I_0. \tag{23}$$

In the DBCP experiments, D values ranged from about 0.0375 to about 4, and in most cases, it was around 0.65. Data analysis shows that all the experimental results and AdOx™ model predictions of hydrogen peroxide degradation can be fit with either a zero or a first order rate expression with

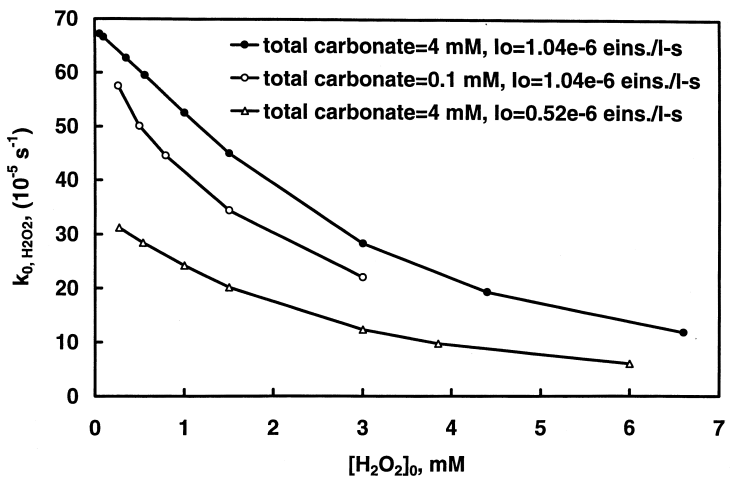

Fig. 5. AdOx model predicted relationship between the initial hydrogen peroxide concentration and the pseudo-first-order rate constant of hydrogen peroxide consumption.

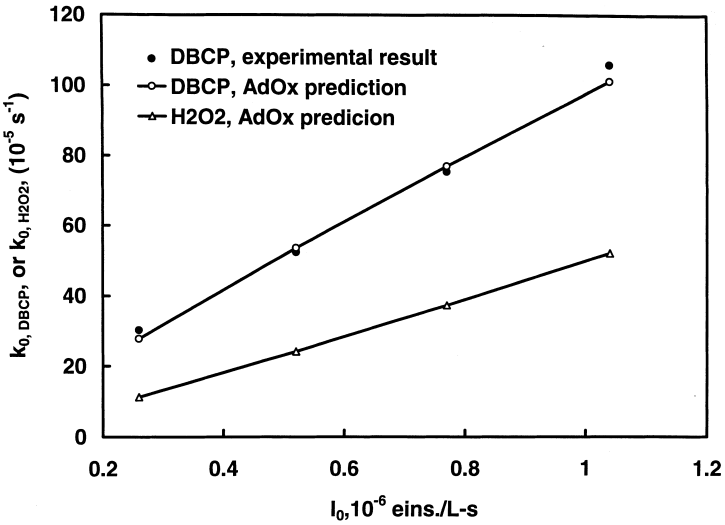

Fig. 6. Effect of incident UV-light intensity on pseudo-first-order rate constants of both DBCP and hydrogen peroxide degradation (operating parameters: $C_{T,CO_3} = 4$ mM; $[H_2O_2]_0 = 1.00$ mM).

high correlation coefficients. A pseudo-first order kinetic rate expression is chosen to study the hydrogen peroxide consumption as it is for the DCBP decomposition.

Figure 5 shows AdOx™ model predictions of the relationship between the pseudo-first order rate constant of hydrogen peroxide consumption and the initial hydrogen peroxide concentration. It indicates that in addition to impacting the degradation rate of DBCP, increasing the initial hydrogen peroxide concentration decreases the pseudo-first order rate constant of hydrogen peroxide consumption. This implies that using excess hydrogen peroxide for the process will not only increase the operating cost, decrease the removal rate of the organic pollutants, but also leave a high hydrogen peroxide residual in the treated water.

Effect of incident UV-light intensity

Figure 6 shows the effect of the incident UV-light intensity on the pseudo-first order degradation rate constants for both DBCP (also see data group IV in Table 2) and hydrogen peroxide. It can be seen that the pseudo-first order degradation rate constants for both DBCP and hydrogen peroxide are proportional to the incident UV-light intensity within the UV-light intensity range studied.

Effect of total inorganic carbonate concentration

Figure 7 shows the effects of the total inorganic carbonate concentration (C_{T,CO_3}) on the pseudo-first-order rate constants of both DBCP (also see data group VI in Table 2) and hydrogen peroxide. Obviously, increasing C_{T,CO_3} decreases the oxidation rate of DBCP significantly. This is because the carbonate species scavenge significant amounts of hydroxyl radicals, as previously discussed. However, a change in C_{T,CO_3} has little effect on the consumption rate of hydrogen peroxide. This is expected because photolysis is the major mechanism for hydrogen peroxide loss.

Effect of pH

Figure 8 shows the effect of initial solution pH on the pseudo-first order rate constants of both DBCP (also see data group VII in Table 2) and

Table 3. Sensitivity analysis: comparison of AdOx™ predictions vs two-assumption model, and constant pH assumption model predictions

$[R_0]$ (μM)	$[H_2O_2]_0$ (mM)	I_0 (eins./l s)	$[C_{T,CO_3}]$ (mM)	pH	k_0 ($\times 10^5$ s^{-1})			
					experiment	two-assumption model	const. pH model	AdOx™ model
1.63	0.054	1.04×10^{-6}	4	8.4	26.5	8.54	33.5	34.3
1.43	0.096	1.04×10^{-6}	4	8.3	30.7	10.3	38.9	39.1
1.42	0.35	1.04×10^{-6}	4	8.4	61.9	16.8	60.9	64.0
1.55	0.56	1.04×10^{-6}	4	8.5	81.5	19.4	71.2	79.0
1.83	1	1.04×10^{-6}	4	8.4	106	24.4	92.6	98.4
1.77	1.5	1.04×10^{-6}	4	8.4	108	25.8	101.1	107.5
1.5	3	1.04×10^{-6}	4	8.4	107	23.7	95.8	101.4
1.52	4.4	1.04×10^{-6}	4	8.4	85.5	20.1	81.2	85.7
3.06	6.6	1.04×10^{-6}	4	8.5	70.9	14.9	59.4	65.8

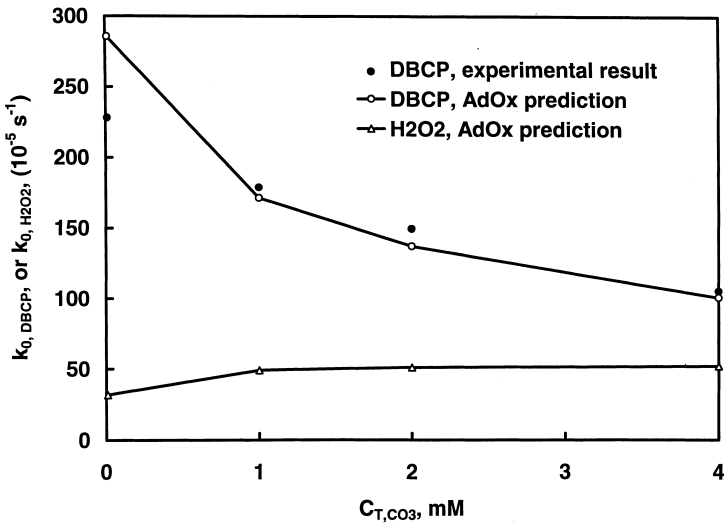

Fig. 7. Effect of total inorganic carbonate concentration on pseudo-first-order rate constants of both DBCP and hydrogen peroxide degradation (operating parameters: $I_0 = 1.04 \times 10^{-6}$ eins./l s; $[H_2O_2]_0 = 1.00$ mM).

hydrogen peroxide. When the total inorganic carbonate concentration is held constant, an increase in initial solution pH decreases the oxidation rate of DBCP significantly. This is because the carbonate ion (CO_3^{2-}) concentration increases with increasing pH, and CO_3^{2-} is a much more effective scavenger of hydroxyl radicals than HCO_3^- (see the second order rate constants in Table 1). In addition, the dissociated form of hydrogen peroxide (HO_2^-) in alkaline media reacts with hydroxyl radicals more than two orders of magnitude faster than hydrogen peroxide does. Higher pH values slightly enhance the decomposition of hydrogen peroxide for the same reason. Furthermore, the molar extinction coefficient of HO_2^- is more than ten times greater than that H_2O_2 (with the same quantum yield as H_2O_2), and thus increases the hydrogen peroxide decomposition.

pH change during reaction, which is caused by Br^-, Cl^-, and CO_2 (H_2CO_3*) formation, is important. When the inorganic carbonate concentration is relatively high ($C_T = 4$ mM), and the solution is well buffered, the AdOx™ model predicts the solution pH only drops about 0.2 unit (for a typical run, pH changes from 8.4 to 8.22). This small pH drops significantly affects the process efficiency because of the change in carbonate/bicarbonate ion distribution. When the inorganic carbonate concentration is low ($C_T \leq 0.1$ mM), AdOx™ predicts pH decreases of 0.63–1.31 units during the process depending on operating conditions, and this impacts process performance in a similar fashion.

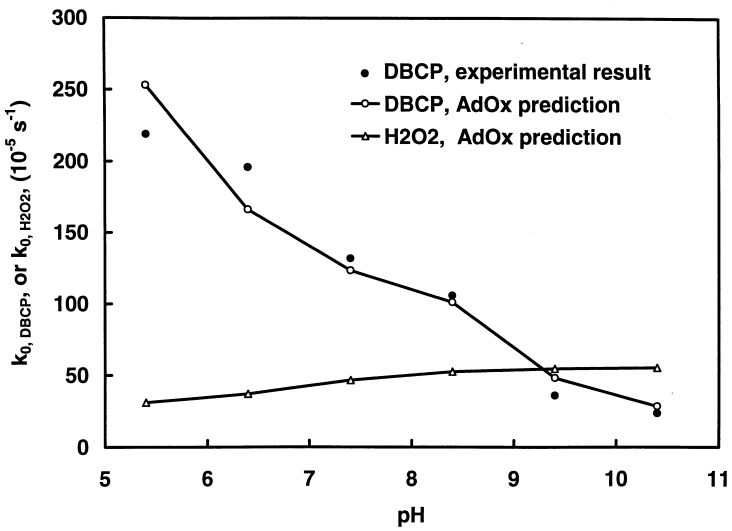

Fig. 8. Effect of solution pH on pseudo-first-order rate constants of both DBCP and hydrogen peroxide degradation (operating parameters: $I_0 = 1.04 \times 10^{-6}$ eins./l s; $[H_2O_2]_0 = 1.00$ mM; $C_{T,CO_3} = 4$ mM).

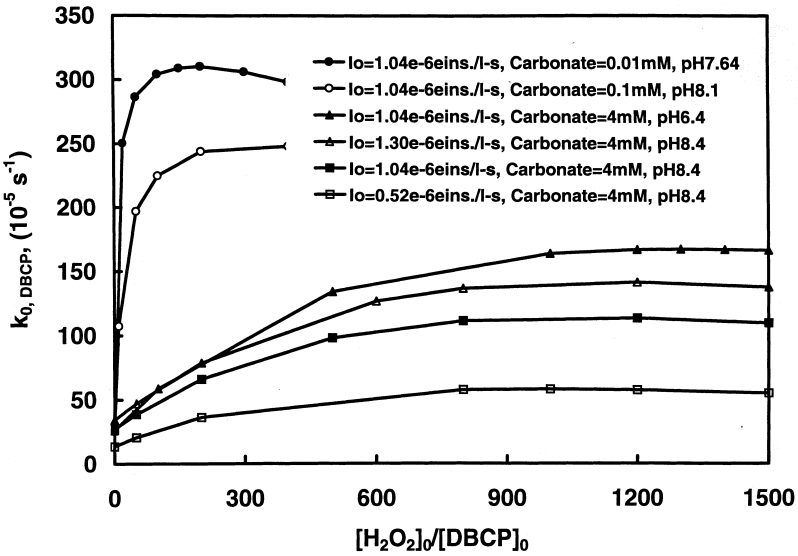

Fig. 9. AdOx model predicted relationship between the molar ratio of $[H_2O_2]_0/[DBCP]_0$ and the pseudo-first-order rate constant of DBCP degradation.

Unfortunately, the experimental pH values were not reported; therefore, the predicted pH values could not be compared to measured values.

Impact of operating parameters on the process efficiency

Figure 9 shows AdOx™ predicted pseudo-first order rate constants of DBCP degradation vs the initial molar ratio of hydrogen peroxide to the organic pollutant compound, DBCP, under various processing conditions. Figure 9 indicates that there is an optimum oxidant to organic compound ratio for the destruction of the organic pollutant. Furthermore, these optimum values and corresponding molar ratio of hydrogen peroxide to the organic compound are greatly affected by process operating parameters such as incident UV-light intensity, the total inorganic carbonate concentration in the solution, and the initial solution pH. Among these process operating parameters, the inorganic carbonate concentration shows the greatest effect on the process efficiency. An economic analysis, such as the EE/O concept introduced by Bolton and Cater (1994), can be used to determine whether carbonate removal (perhaps by softening), pH adjustment, or increasing UV-light intensity is cost effective for a given situation.

Bolton and Cater (1994) introduced a "figure of merit", electrical energy per order (EE/O), to evaluate the cost efficiency of photodegradation water treatment processes. This "figure of merit" (EE/O) is defined as the electrical energy (in kWh) required to reduce the concentration of a pollutant by one order of magnitude in 1000 U.S. gallons (3785 l) of water. The EE/O value for a CMBR may be calculated from the following equation:

$$\mathrm{EE/O} = \frac{P \times (t/3600) \times 3785}{V \times \log[C_0/C]} = \frac{2.42P}{Vk_0}\ (\mathrm{kWh/kgallon\text{-}order}), \qquad (24)$$

in which P is the lamp power (kW), t is the irradiation time (s), V is the reactor volume (l), C_0 is the initial concentration of the pollutant, C is the final concentration of pollutant at the end of the UV irradiation, and k_0 is the pseudo-first order rate constant of the organic compound degradation (1/s). According to Bolton and Cater (1994), EE/O values of 10 or less are considered favorable.

The EE/O values for the DBCP oxidation process can be estimated according to the preceding equation. Unfortunately, the electrical power of the UV lamps was not directly reported (Lay, 1989; Glaze *et al.*, 1995). However, the UV intensity at 254 nm was measured to be 8.4 w for each lamp (or expressed as 0.12 w/l each, or 0.26×10^{-6} eins./l s each). Assuming an electrical efficiency of 30% (Bolton and Cater, 1994), the EE/O values are calculated and reported in Table 2. It indicates that applying an optimum hydrogen peroxide dosage, reducing inorganic carbonate concentration, and adjusting pH value to a lower level can reduce the EE/O value. Obviously, increasing UV-light intensity, which corresponds to higher electrical energy consumption, is not the best way to increase the pollutant removal rate since it may increase the EE/O value.

CONCLUSIONS

A dynamic kinetic model (AdOx™) for the advanced oxidation process using the combination of hydrogen peroxide and ultraviolet irradiation in a completely mixed batch reactor (CMBR) has been

developed in this work. The AdOx™ model is based on known elementary chemical and photochemical reactions. Literature reported photochemical parameters and chemical reaction rate constants are used in this model to describe the kinetic rates of all the main species in the solution, and to predict the organic compound destruction. The effects of water quality, such as the presence of carbonate and bicarbonate ions, pH, as well as the presence of humic substances, on the process efficiency are considered in AdOx™ (although, only the results for organic-free water is presented here). Unlike most other kinetic models of H_2O_2/UV oxidation process, AdOx™ does not assume that the net formation rate of free radical species is zero (pseudo-steady state assumption). It also considers the pH decrease during the process as mineral acids and carbon dioxide are formed. The model provides a comprehensive understanding of the impact of design and operational variables, such as initial hydrogen peroxide concentration and UV-light intensity on process performance, and these design and operational variables can be optimized using the model.

The following conclusions may be drawn from the model verification:

1. The AdOx™ model that does not employ pseudo-steady state assumption and constant pH assumption gives a better prediction of the destruction of target organic compound than a model that uses these assumptions.
2. The presence of inorganic carbonate ions greatly decreases the efficiency of the H_2O_2/UV process because they scavenge hydroxyl radicals.
3. There exists an optimum hydrogen peroxide dosage for each set of reactor conditions with regard to the organic pollutant removal efficiency of the H_2O_2/UV process.

Acknowledgements—This research is based upon work supported by the Center for Clean and Industrial and Treatment Technologies (CenCITT) sponsored by the U.S. Environmental Protection Agency, and the Environmental Engineering Center for Water and Waste Management at Michigan Technological University. Any opinions, findings, conclusions or recommendations expressed in this publication are those of the authors and do not necessarily reflect the view of the supporting organizations.

REFERENCES

Baxendale J. H. and Wilson J. A. (1957) The photolysis of hydrogen peroxide at high light intensities. *Trans. Faraday Soc.* **53,** 344–356.

Beck (1969) Detection of charged intermediate of pulse radiolysis by electrical conductivity measurements. *Int. J. Radiat. Phys. Chem.* **1**(3)**,** 361–371.

Bielski H. J., Benon H. J., Cabelli D. E., Ravindra L. A. and Alberta A. B. (1985) Reactivity of perhydroxyl/superoxide radicals in aqueous solution. *J. Phys. Chem. Ref. Data* **14**(4)**,** 1041–100.

Bolton J.R. and Cater S.R. (1994) Homogeneous photodegradation of pollutants in contanminated water: an introduction. *Aq. Surf. Photochem.* **0,** 467–490.

Braun W., Herron J. T. and Kahanner D. K. (1988) Auchem: a computer program for modeling complex chemical reaction systems. *Int. J. Chem. Kin.* **20,** 51–62.

Buxton G. V., Greenstock C. L., Helman W. P. and Ross A. B. (1988) Critical review of rate constants for reactions of hydrated dlectrons, hydrogen atoms and hydroxyl radicals (AOH/AO^-) in aqueous solution. *J. Phys. Chem. Ref. Data* **17**(2), 513–886.

Chen S. N. and Hoffman M. Z. (1975) Effect of pH on the reactivity if the carbonate radical in aqueous solutions. *Radiat. Res.* **62,** 18–27.

Christensen H. S., Sehested K. and Corftizan H. (1982) Reaction of hydroxyl radicals with hydrogen peroxide at ambient temperatures. *J. Phys. Chem.* **86,** 15–88.

De Laat J. and Dore M. (1994) Degradation of chloroethanes in dilute aqueous solution by H_2O_2/U.V.. *Wat. Res.* **28**(12), 2507–2519.

Draganic Z. D., Negron-mendoza A., Sehested K., Vujosevic S. I., Navarro-Gonzales R., Albarran-Sanchez M. G. and Draganic I. G. (1991) Radiolysis of aqueous solutions of ammonium bicarbonate over a large dose range. *Radiat. Phys. Chem.* **38**(3)**,** 317–21.

Eriksen T. E., Lind J. and Merenyi G. (1985) On the acid–base equilibrium of the carbonate radical. *Radiat. Phys. Chem* **26**(2)**,** 197–199.

Glaze W.H. and Kang J.W. (1988) Advanced oxidation processes for treating groundwater contaminated with TCE and PCE: laboratory studies. *J. AWWA* **May,** 57–63.

Glaze W. H. and Kang J. W. (1989a) Advanced oxidation processes. Description of a kinetic model for the oxidation of hazardous materials in aqueous media with ozone and hydrogen peroxide in the semibatch reactor. *Ind. Eng. Chem. Res.* **28,** 1573–1580.

Glaze W. H. and Kang J. W. (1989b) Advanced oxidation processes. Test of a kinetic model for the oxidation of organic compounds with ozone and hydrogen peroxide in a semibatch reactor. *Ind. Eng. Chem. Res.* **28,** 1580–1587.

Glaze W. H., Beltran F., Tuhkanen T. and Kang J. W. (1992) Chemical models of advanced oxidation processes. *Water Poll. Res. J. Canada* **27**(1), 23–42.

Glaze W. H., Lay Y. and Kang J. W. (1995) Advanced oxidation processes. A kinetic model for the oxidation of 1,2-dibromo-3-chloropropane in water by the combination of hydrogen peroxide and UV radiation. *Ind. Eng. Chem. Res.* **34,** 2314–2323.

Hindmarsh A. C. (1974) GEAR: Ordinary Differential Equation System Solver, Lawrence Livermore Laboratory, Report UCID-30001, Revision 3.

Holeman J., Bjergbakke E. and Sehested K. (1987) The importance of radical–radical reactions in pulse radiolysis of aqueous carbonate/bicarbonate. *Proc. Tihany Symp. Radiat. Chem.* **6**(1)**,** 149–53.

Hong A., Zappi M. E., Kuo C. H. and Hill D. (1996) Modeling kinetics of illuminated and dark advanced oxidation processes. *J. Environ. Eng.* **Jan.,** 58–62.

Hu S. (1997) The development of a kinetic model for the H_2O_2/UV AOP and modeling case studies. M.S. thesis, Michigan Technological University.

Huie R. E. and Clifton C. L. (1990) Temperature dependence of the rate constants for reactions of the sulfate radical, SO_4^-, with anions. *J. Phys. Chem.* **94**(23)**,** 8561–8567.

Hunt J. P. and Taube H. (1952) The photochemical decomposition of hydrogen peroxide. Quantum yields, tracer and fractionation effects. *J. Am. Chem. Soc.* **74,** 5999–6002.

Koppenol W. H., Butler J. and Van Leeuwen J. W. L. (1978) The Haber–Weiss Cycle. *Photochem. Photobiol.* **28,** 655–660.

Larson R. A. and Zepp R. G. (1988) Reactivity of the carbonate radical with aniline derivatives. *Environ. Toxicol. Chem.* **7,** 265–274.

Lay Y. S. (1989) Oxidation of 1,2-dibromo-3-chloropropane in groundwater using advanced oxidation processes. Ph.D. dissertation, University of California, Los Angeles.

Liao C. H. (1993) The investigation of hydrogen peroxide photolysis as a water treatment process. Ph.D. dissertation, Drexel University.

Liao C. H. and Gurol M. D. (1995) Chemical oxidation by photolytic decomposition of hydrogen peroxide. *Environ. Sci. Technol.* **29,** 3007–3014.

Mallard W. G., Ross A. B. and Helman W. P. (1992) NIST Standard Reference Database 40, NDRL/NIST Solution Kinetics Database Version 1.0. Data compiled and evaluated by A. B. Ross, B. H. J. Bielski, G. V. Buxton, D. E. Cabelli, C. L. Greenstock, W. P. Helman, R. E. Huie and P. Neta.

Maruthamuthu P. and Neta P. (1978) Phosphate radicals. Spectra, acid–base equilibria, and reactions with inorganic compounds. *J. Phys. Chem.* **82,** 710–713.

Milano J. C., Bernat-Escallon C. and Vernet J. L. (1990) Photolysis of 1,2-dibrono-3-chloropropane in water. *Water Res.* **24**(5), 557–564.

Nakashima M. and Hayon E. (1970) Rates of reaction of inorganic phosphate radicals in solution. *J. Phys. Chem.* **74**(17)**,** 3290–3291.

Perry R. H., Green D. W. and Maloney J. D. (1981) *Chemical Engineer's Handbook* 5th edn. McGraw-Hill, New York.

Peyton G. R. (1990) Guidelines for the selection of a chemical model for advanced oxidation processes. *A symposium on advanced oxidation processes for the treatment of contaminated water and air (proceedings)*, June 4 and 5, 1990, Toronto.

Peyton G. R. and Glaze W. H. (1988) Destruction of pollutants in water with ozone in combination with ultraviolet radiation. 3. Photolysis of aqueous ozone. *Environ. Sci. Technol.* **22,** 761–767.

Peyton G. R., Smith M. A. and Peyton B. M. (1987) Photolytic ozonation for protection and rehabilitation of groundwater resources; a mechanistic study. Report.

Schested K., Rasmussen O. L. and Fricke H. (1968) Rate constants of OH with HO_2,O_2^- and $H_2O_2^+$ from hydrogen peroxide formation in pulse-irradiated oxygenated water. *J. Phys. Chem.* **72,** 626–631.

Stefan M. I., Hoy A. R. and Bolton J. R. (1996) Kinetics and mechanism of the degradation and mineralization of acetone in dilute aqueous solution sensitized by the UV photolysis of hydrogen peroxide. *Environ. Sci. Technol.* **30,** 2382–2390.

Stumm W. and Morgan J. J. (1972) *Aquatic Chemistry*, Prentice-Hall, Engelwood, NJ.

Volman D. H. and Chen J. C. (1959) The photochemical decomposition of hydrogen peroxide in aqueous solutions of allyl alcohol at 2537 Å. *J. Am. Chem. Soc.* **81,** 4141–4144.

Weinstein J., Benon H. J. and Bielski H. J. (1979) Kinetics of the interaction of HO_2 and O_2^- radicals with hydrogen peroxide. The Haber–Weiss reaction. *J. Am. Chem. Soc.* **101,** 58–62.

Weir B. A. and Sundstrom D. W. (1993) Destruction of trichloroethylene by UV light-catalyzed oxidation with hydrogen peroxide. *Chemosphere* **27**(7), 1279–1291.

Yao C. D., Haag W. R. and Mill T. (1992) Kinetic features of advanced oxidation processes for treating aqueous chemical mixtures. *Chemical Oxidation, Technology for the Nineties*, Nashville, TN, 19–21 Feb. 1992.